Journal of Helminthology

www.cambridge.org/jhl

Steinernema shori n. sp., a new entomopathogenic nematode (Nematoda: Steinernematidae) from India

S. Soni[1,*], J. Patil[2,*], V. Linga[2], P.H. Mhatre[3], M.T. Gowda[4], J. Ganguli[1] and V. Půža[5]

[1]Indira Gandhi Krishi Vishwavidyalaya, Raipur–492012, Chhattisgarh, India; [2]Indian Council of Agricultural Research (ICAR)–National Bureau of Agricultural Insect Resources, Bengaluru–560024, Karnataka, India; [3]ICAR–Central Potato Research Station, Udhagamandalam, Nilgiris–643004, Tamil Nadu, India; [4]ICAR–Indian Institute of Vegetable Research, Varanasi–221305, Uttar Pradesh, India and [5]Biology Centre of the Czech Academy of Sciences, Institute of Entomology, Branišovská 1160/31, 370 05 Ceské Budejovice, Czech Republic

Research Paper

Cite this article: Soni S, Patil J, Linga V, Mhatre PH, Gowda MT, Ganguli J and Půža V (2023). *Steinernema shori* n. sp., a new entomopathogenic nematode (Nematoda: Steinernematidae) from India. *Journal of Helminthology*, **97**, e72, 1–14
https://doi.org/10.1017/S0022149X23000536

Received: 13 July 2023
Revised: 15 August 2023
Accepted: 15 August 2023

Keywords:
Description; molecular characterization; phylogenetic systematics; *Steinernema*; taxonomy; India

Corresponding author:
J. Patil;
Email: patiljaggi@gmail.com

*Joint first authors.

Abstract

In this study, morphological and molecular features were used to identify a new *Steinernema* sp. from Chhattisgarh, India. Morphological and molecular features provide evidence for placing the new species into the "*bicornutum*" clade. The new species is characterized by the following morphological features: infective juveniles with a body length of 587 (494–671) µm; a distance from the anterior end to excretory pore of 46 (43–50) µm; a distance from anterior end to nerve ring of 72 µm (61–85 µm); and *E*% of 88 (77–97). The first-generation males are characterised by 27 genital papillae and very short spicules, with a length of 61 µm (53–67) µm. The *SW*% and *GS*% ratio of *S. shori* n. sp. are 139 (107–190) and 75 (62–90), respectively. The new species is further characterized by sequences of the internal transcribed spacer and partial 28S regions of the ribosomal DNA. Phylogenetic analyses show that *S. shori* n. sp. is most closely related to *S. abbasi, S. kandii,* and *S. yirgalemense.*

Introduction

Entomopathogenic nematodes (EPN) belonging to the families Heterorhabditidae and Steinernematidae are obligate parasites of insects, mutualistically associated with bacteria of genera *Photorhabdus* spp. for heterorhabditids and *Xenorhabdus* spp. for steinernematids. They possess many qualities that make them excellent biological control agents. Therefore, their economic importance is increasing. Steinernematids have a worldwide distribution, and so far, more than 100 species have been described, identified on all continents except Antarctica, and this number is growing every year. They have been used successfully for the management of economically important insect pests (Hominick 2002; Půža 2015).

The steinernematid nematodes collected within the present study possess infective larvae with two horn-like structures on the labial region, which is a typical trait of species of the "*bicornutum*" group. Presently, this group includes 12 described species: *S. riobrave* Cabanillas, Poinar and Raulston 1994 (from Texas, USA); *S. bicornutum* Tallósi Peters and Ehlers 1995 (from Yugoslavia); *S. abbasi* Elawad, Ahmad and Reid 1997 (from Oman); *S. ceratophorum* Jian, Reid and Hunt 1997 (from Northeast China); *S. pakistanense* Shahina, Anis, Reid, Rowe and Maqbool 2001 (from Pakistan); *S. yirgalemense* Nguyen, Tesfamariam, Gozel, Gaugler and Adams 2004 (from Ethiopia); *S. bifurcatum* Fayyaz, Yan, Qui, Han, Gulsher, Khanum and Javed 2014 (from Pakistan); *S. papillatum* San-Blas, Portillo, Nermut′, Půža and Morales-Montero 2015 (from Venezuela); *S. biddulphi* Çimen, Půža, Nermut′, Hatting, Ramakuwela and Hazir 2016 (from South Africa); *S. goweni* San-Blas, Morales-Montero, Portillo, Nermut′ and Půža 2016 (from Zulia State, Venezuela); *S. ralatorei* Grifaldo-Alcantara, Alatorre-Rosas, Segura-León and Hernandez-Rosas 2017 (from a sugarcane area in Mexico), and *S. kandii* Godjo, Afouda, Baimey, Couvreur, Zadji, Houssou, Bert, Willems and Decraemer 2019 (from northern Benin).

In 2021 a survey was conducted in Chhattisgarh, India to determine the occurrence and distribution of EPN. The survey resulted in the recovery of three isolates of EPN, with only one undescribed *Steinernema* species detected from the rhizosphere of a Sal (*Shorea robusta*) plantation. Morphological, morphometric, and molecular data prove that *Steinernema* type strain NBAIRS80 isolated in the present study is a new species. The new species is described herein as *S. shori* n. sp. This will be the third *Steinernema* species described from India; previously, *S. indicum* Patil, Linga, Mhatre, Gowda, Rangasamy and Půža 2023 and *S. anantnagense* Bhat, Machado, Abolafia, Askary, Půža, Ruiz-Cuenca, Ameen, Rana, Sayed and Al-Shuraym 2023 have been described from India.

© The Author(s), 2023. Published by Cambridge University Press.

Materials and methods

Nematode isolation and rearing

Soil samples were collected during October 2021 from a Sal (*Shorea robusta*) plantation at Jagdalpur (19°5′8″N, 81°57′35″E) city of the Bastar district in Chhattisgarh state, India. Each sample contained 5–10 subsamples, which were randomly taken at least 8–10 m apart, from the surface to a depth of 15 cm. The subsamples were pooled and placed in a plastic bag, mixed, and transported to the laboratory (Bedding & Akhurst 1975). The soil type was sandy clay loam. Five last instar *Galleria mellonella* (L.) larvae were placed in a 500 ml plastic container and then filled with moistened soil from each sample. *Galleria* larval mortality was recorded on a daily basis. Dead larvae were placed into White traps (White 1927), and infective juveniles were collected and used to infect live *G. mellonella* larvae to confirm Koch's postulates (Kaya & Stock 1997). For taxonomic studies, 30 *G. mellonella* were exposed to infective juveniles (IJ) (200 IJ per *G. mellonella*) of nematodes in a 9.0 cm diameter Petri dish lined with a moistened filter paper and kept in the dark at 28 ± 2°C. First- and second-generation adult nematodes were obtained at 3 and 6 days, respectively, after the death of *Galleria* larvae by dissecting the *G. mellonella* cadavers in Ringer's solution. Infective juveniles were obtained upon emergence from the cadavers 8 days after the death of *Galleria* larvae.

Differential interference contrast microscopy

For light microscopy, the specimens of different stages were heat-killed, fixed in formaldehyde-glycerine fixative (Hooper 1970) for 24 h and then transferred to glycerine-alcohol (5 parts glycerine: 95 parts 30% alcohol; Seinhorst 1959) for slow dehydration in a desiccator. Dehydrated specimens were mounted in anhydrous glycerine on glass slides using the wax ring method (De Maeseneer & D'Herde 1963). Morphometric analysis of the nematode specimens was done for 20 individuals of the adult stages of both generations and IJs, using a Carl Zeiss Axio imager Z2 microscope fitted with DIC optics (Jena, Germany), a digital camera (Zeiss Axiocam 503 colour camera), and the image analysing software Zen 2 Blue edition.

Scanning electron microscopy (SEM)

Adults of both generations were dissected from *G. mellonella* larvae in Ringer's solution (pH 7.3). They were rinsed three times for 3 min in Ringer's solution. All the nematodes were heat-killed and then fixed in 4% formalin buffered with 0.1 M phosphate buffer at pH 7.2 for 24 h at 4–6°C. They were post-fixed with a 2% osmium tetroxide solution for 12 h at 25°C and then dehydrated at 15 min intervals through 20%, 30%, 50%, 70%, 90%, 95%, and 100% ethanol. They were then critical point-dried with liquid CO_2, mounted on SEM stubs, and coated with gold (Nguyen & Smart 1995, 1997). The mounts were examined with a Carl Zeiss EVO-18 scanning electron microscope (Jena, Germany).

Molecular characterization

DNA was extracted from single female. Each female was transferred into a sterile Eppendorf tube (1.5 ml) with 20 µl of extraction buffer (17.7 µl of ddH2O, 2 µl of 10 × PCR buffer, 0.2 µl of 1% Tween, and 0.1 µl of proteinase K (20 mg/ml). Buffer and nematode were frozen at −20°C for 20 min and then immediately incubated at 65°C for 1 h, followed by 5 min at 95°C. The lysates were cooled on ice, centrifuged (2 min, 9000 *g*), and 1 µl of supernatant was used for PCR. Primers were synthesised by Bioserve Biotechnologies Pvt. Ltd (Telangana, India). A fragment of rDNA containing the internal transcribed spacer regions (ITS1, 5.8S, ITS2) was amplified using primers 18S: 5′-TTGATTACGTCCCTGCCCTTT- 3′ (forward) and 28S: 5′-TTTCACTCGCCGTTACTAAGG-3′ (reverse) (Vrain *et al.* 1992). The other fragment containing D2–D3 expansion segments of the 28S rDNA gene was amplified using primers D2F: 5′-CCTTAGTAACGGCGAGTGAAA-3′ (forward) and 536: 5′-CAGCTAT CCTGAGGAAAC-3′ (reverse) (Nguyen 2007), and the cytochrome oxidase I (COI) was amplified using primers COIF1: 5′-CCTACTATGATTGGTGGTTTTGGTAATTG-3′ (forward) and COIR2: 5′-GTAGCAGCAGTAAAATAAGCACG-3′ (reverse) (Kanzaki & Futai 2002). PCR reactions consisted of 1 µl of genomic DNA, 15.25 µl of EmeraldAmp GT PCR master mix (Takara Bio, Shiga, Japan), 0.75 µl of both forward and reverse primers, and 7.25 µl of dH2O. The PCR profiles were used as follows for ITS: 1 cycle of 95°C for 5 min followed by 35 cycles of 94°C for 60 s, 55.4°C for 30 s, 72°C for 60 s, and a final extension at 72°C for 10 min; for 28S rDNA: 1 cycle of 95°C for 5 min followed by 35 cycles of 94°C for 60 s, 50°C for 30 s, 72°C for 60 s, and a final extension at 72°C for 10 min; and for COI: 1 cycle of 95°C for 5 min followed by 35 cycles of 94°C for 60 s, 50°C for 30 s, 72°C for 60 s, and a final extension at 72°C for 10 min. PCR was followed by electrophoresis (120 min 70 V) of 2 µl of PCR product in a 1% TAE-buffered agarose gel stained with ethidium bromide (10 µl ETB per 100 ml of gel). The PCR products were sequenced by Eurofins Genomics (Karnataka, India). The PCR products were sequenced and deposited in GenBank with accession numbers OR194554 (ITS sequences), OR194555 (28S sequence), and OR187856 (COI sequence).

Entomopathogenic bacteria isolation and molecular characterization

The bacteria were obtained from the haemolymph of *G. mellonella* 1 day after infection with *Steinernema* sp. type strain NBAIRS80 by using the method of Akhurst (1980). The haemolymph was streaked on nutrient agar supplemented with 0.004% (w/v) triphenyltetrazolium chloride and 0.0025% (w/v) bromothymol blue (NBTA medium) and left 2 days at 28°C (Akhurst 1980). Single colonies were transferred with a sterile toothpick to YS broth (Akhurst 1980) and cultivated on an orbital shaker (180 rpm) at 25°C. Bacterial DNA was extracted from a two-day-old culture using a DNeasy Blood and Tissue Kit (Qiagen, Hilden, Germany) according to the manufacturer's instructions. 16S RNA was amplified using primers fD1: 5′-GAGTTTGATCCTGGCTCA-3′ (forward), and rP2: 5′-ACGGCTACCTTGTTACGACTT-3′ (reverse) (Weisburg *et al.* 1991). Recombinase A gene (*recA*) was amplified using primers RecA1F: 5′-GCTATTGATGAAAATAAACA-3′ (forward) and RecA2R: 5′-RATTTTRTCWCCRTTRTAGCT-3′ (reverse) (Tailliez *et al.* 2010). Gyrase B gene (*gyrB*) was amplified using primers 1200F gyrB: 5′- GATAACTCTTATAAAGTTTCCG-3′ (forward) and 1200R gyrB: 5′- CGGGTTGTATTCGTCACGGCC-3′ (reverse) (Tailliez *et al.* 2010). PCR reactions consisted of 1 µl of genomic DNA, 15.25 µl of EmeraldAmp GT PCR master mix (Takara Bio, Shiga, Japan), 0.75 µl of both forward and reverse primers, and 7.25 µl of dH2O. The PCR profiles were used as follows for 16S: 1 cycle of 94°C for 1 min followed by 33 cycles of 94°C for 60 s, 55°C for 60 s, 72°C for 2 min, and a final extension at 72°C for 3 min, *recA*: 1 cycle at 94°C for 2 min followed by 35 cycles at 94°C for 30 s, 49.5°C for 35 s, 72°C for 60 s, and a final extension at 72°C for 2 min, and for *gyrB*: 1 cycle at 94°C for 2 min followed by 35 cycles at 94°C for 30 s, 56.5°C for 35 s, 72°C for 60 s, and a final extension at 72°C for 2 min. The PCR

https://doi.org/10.1017/S0022149X23000536 Published online by Cambridge University Press

products were sequenced by HiMedia (HigenoMB, Mumbai, India). The PCR products were sequenced and deposited in GenBank under the following accession numbers OR187299 (16S sequence), OR232178 (*recA* sequence), and OR232179 (*gyrB* sequence).

Phylogenetic analysis

The newly obtained ribosomal DNA sequences of the ITS and D2–D3 regions of 28S were deposited in the GenBank (Altschul *et al.* 1997) (Table S1). The sequences were edited and compared with those present in GenBank by means of a Basic Local Alignment Search Tool (BLAST) from the National Center for Biotechnology Information (NCBI). An alignment of the samples with sequences of species of the "*bicornutum*" group was produced for each amplified DNA region using default ClustalW parameters in MEGA 7.0 (Kumar *et al.* 2016) and optimised manually in BioEdit (Hall 1999). Pairwise distances were computed using MEGA 7.0 (Kumar *et al.* 2016).

Phylogenetic trees were obtained by the Minimum Evolution method (Rzhetsky & Nei 1992) in MEGA 7.0 (Kumar *et al.* 2016). *Steinernema nepalense* Khatri-Chhetri, Waeyenberge, Spiridonov, Manandhar and Moens, 2011 and *S. scapterisci* Nguyen and Smart 1990 were used as outgroup taxa. The Minimum Evolution tree was searched using the Close-Neighbour-Interchange (CNI) algorithm (Nei & Kumar 2000). The neighbour-joining algorithm (Saitou & Nei 1987) was used to generate the initial tree. Evolutionary distances were computed using the p-distance method (Nei & Kumar 2000) and are expressed as the number of base differences per site.

Results

Description of *Steinernema shori* n. sp. (Figures 1–3)

Measurements

The dimensions of the holotype and paratype specimens are provided in Table 1.

Description

Infective juvenile. Body slender, tapering gradually from base of pharynx to anterior end and from anus to terminus. Average body length 587 µm (Table 1), second stage cuticle sheath present after emergence from the host. Body almost straight or slightly

Table 1. Morphometrics of *Steinernema shori* n. sp. All measurements are in µm and in the form: mean ± s.d. (range)

	First generation			Second generation		Infective juveniles
	Male		Female	Male	Female	
Character	Holotype	Paratypes	Paratypes	Paratypes	Paratypes	Paratypes
n	–	20	20	20	20	20
L	1596	1592 ± 134	5912 ± 954	924 ± 102	1331 ± 151	587 ± 50
		(1923–1388)	(3772–7973)	(729–1114)	(1671–1741)	(494–671)
a	12	10 ± 0.8	25 ± 3	17 ± 2	17 ± 2	23 ± 1
		(8–12)	(20–32)	(12–21)	(15–20)	(20–26)
b	11.7	11.2 ± 1.0	35.9 ± 6	8 ± 0.8	10.2 ± 1.1	5.8 ± 0.4
		(9.4–13)	(23.7–49.2)	(6.6–9.6)	(8.3–12.5)	(5.1–6.7)
c	6361	58 ± 6.7	228 ± 53	53 ± 8	36 ± 5	11 ± 1
		(44–69)	(139–343)	(44–77)	(27–45)	(10–12)
c′	0.6	0.6 ± 0.1	0.6 ± 0.2	0.6 ± 0.1	1.2 ± 0.1	3.7 ± 0.3
		(0.5–0.8)	(0.4–1.4)	(0.5–0.7)	(1–1.5)	(3.2–4.4)
V%	–	–	50 ± 3	–	583 ± 4	–
		(44–54)			(61–62)	
Max. body diam. (W)	136	158 ± 20.5	239 ± 30	55 ± 4.4	80 ± 11	26 ± 2
		(134–207)	(153–279)	(47–65)	(58–102)	(23–30)
Anterior end to excretory pore (EP)	76	73 ± 8.5	61 ± 13	64 ± 4.4	64 ± 5	46 ± 2
		(60–91)	(37–88)	(51.4–72.6)	(57–73)	(43–50)
Pharynx (ES)	136	143 ± 5.6	165 ± 8	115 ± 4.8	131 ± 8	102 ± 6
		(156–187)	(152–178)	(107–123)	(109–141)	(93–116)
Testis Reflection	183	353 ± 92.5	–	162 ± 23.5	–	–
		(128–150)		(119–203)		
Tail (T)	26	28 ± 2.2	27 ± 5	18 ± 2	37 ± 4	52 ± 4
		(23–33)	(19–39)	(13–22)	(30–44)	(45–61)
Anal body diam. (ABD)	44	45 ± 5	44 ± 9	29 ± 1.6	31 ± 2	14 ± 1
		(34–52)	(29–61)	(25–35)	(26–35)	(12.16)

(*Continued*)

https://doi.org/10.1017/S0022149X23000536 Published online by Cambridge University Press

Table 1. (*Continued*)

Character	First generation			Second generation		Infective juveniles
	Male		Female	Male	Female	
	Holotype	Paratypes	Paratypes	Paratypes	Paratypes	Paratypes
Spicule (SL)*	62	61 ± 4	–	56 ± 4.7	–	–
		(53–67)		(46–65)		
Gubernaculum (GL)	43	46 ± 5.2	–	44 ± 5	–	–
		(37–54)		(33–52)		
Anterior end to vulva	–	–	2997 ± 600	–	769 ± 114	–
			(1894–4177)		(435–999)	
Anterior end to nerve ring	105	101 ± 6.3	115 ± 11	90 ± 8.2	95 ± 12	72 ± 5
		(85–112)	(95–129)	(65–105)	(65–109)	(61–85)
Hyaline tail length (HT)	–	–	–	–	–	30 ± 3
						(25–35)
Tail diam. at start of hyaline region	–	–	–	–	–	7 ± 1
						(5–9)
Rectum	–	–	40 ± 6	–	28 ± 4	25 ± 4
			(30–52)		(21–34)	(19–30)
D% (EP/ES × 100)	56	51 ± 6.3	37 ± 9	56 ± 5	49 ± 4	45 ± 2
		(42–63)	(21–54)	(46–63)	(41–58)	(43–50)
E% (EP/T × 100)	293	264 ± 44.1	233 ± 56	369 ± 61	179 ± 19	88 ± 5
		(198–358)	(103–313)	(294–529)	(142–201)	(77–97)
SW% (SL/ABD × 100)	141	139 ± 20.9	–	195 ± 18	–	–
		(107–190)		(1629–235)		
GS% (GL/SL × 100)	69	75 ± 7.3	–	79 ± 9	–	–
		(62–90)		(64–97)		
H% (HT/T × 100)	–	–	–	–	–	58 ± 3
						(80–105)
Mucron	–	–	–	5 ± 1	–	–
				(3.1–6.9)		

*Measuring along the chord

bow shaped when heat-killed. Labial region smooth, continuous with body. Exsheathed IJ with two horn-like structures on labial region, very distinct by light microscopy and SEM, four distinct cephalic papillae and a pair of pore-like amphidial apertures located laterally (Figure 2a). Cuticle with prominent striations (distinct under SEM) *ca* 2 µm wide at mid-body. Deirids not observed. Hemizonid visible, located just posterior to the nerve ring. Stoma closed, pharynx corpus slender, cylindrical, isthmus distinct, surrounded by nerve ring (Figure 3a). Excretory pore located anterior to midpharynx (*D*% = 45) (Table 1). Cardia present (Figure 3a). Bacterial vesicle usually not well seen. Rectum long, anus distinct. Lateral fields consisting of six ridges in mid-body region (i.e. seven lines) (Figure 2b). Lateral field beginning anteriorly with a cuticular depression (line) on the 1st annulus; at 17th annulus, two ridges appearing and changing to six ridges (seven lines) at excretory pore level. Close to anus, lateral field reducing to two ridges extending almost to tail tip (Figure 2c). Formula of lateral field: 2, 6, 2. Rectum long, anus distinct (Figure 3b). Tail conoid with pointed terminus. Hyaline portion occupying 58% of tail length (Figure 3b). Phasmids clearly visible only in SEM.

First-generation male. Body curved ventrally posteriorly, C- or J-shaped when heat-relaxed (Figure 1l). Cuticle smooth under light microscopy (Figures 3c, d), but with faint transverse striations visible under SEM (Figure 2h). Head round and continuous with body. Face with six labial and four cephalic papillae. Amphidial apertures visible with SEM, located posterior to lateral labial papillae. Stoma shallow, narrow, and usually cuticularized. Pharynx with cylindrical procorpus and slightly swollen metacorpus. Nerve ring usually surrounding isthmus or anterior part of basal bulb. Cardia prominent. Excretory pore located anterior to nerve ring (*ca* 51% of distance from anterior body end to base of pharynx) (Table 1). Testis monorchic, reflexed, consisting of germinal growth zone leading to seminal vesicle. Spicules paired (Figure 3j), curved, golden-brown in colour, *ca* 61 µm long, spicule tip sharp. Manubrium of spicule, usually elongate (manubrium length/manubrium

https://doi.org/10.1017/S0022149X23000536 Published online by Cambridge University Press

Table 2. Comparison of morphometrics of infective juveniles of *Steinernema shori* n. sp. with other members of *bicornutum*-group. All data are in μm and in the form: mean (range). Abbreviations as defined in Table 1

Species	L	MBD	EP	NR	ES	Tail	a	b	c	D%	E%	n
S. shori n. sp.	587	26	46	72	102	52	23	5.8	11	45	88	20
	(494–671)	(23–30)	(43–50)	(61–85)	(93–116)	(45–61)	(20–26)	(5.1–6.7)	(10–12)	(43–50)	(77–97)	
S. abbasi	541	29	48	68	89	56	18	6	10	53	86	–
	(496–579)	(27–30)	(46–51)	(64–72)	(85–92)	(52–61)	(17–20)	(5.5–6.6)	(9–11)	(51–58)	(79–94)	
S. bicornutum	769	29	61	92	124	72	27	6.2	11	50	80	20
	(648–873)	(25–33)	(53–65)	(88–100)	(113–135)	(63–78)	(23–29)	(5.6–6.9)	(10–12)	(40–60)	(80–100)	
S. biddulphi	663	27	55	92	118	58	24	5.6	12	46	95	20
	(606–778)	(24–30)	(51–64)	(84–103)	(111–126)	(53–62)	(21–27)	(5.1–6.2)	(10–13)	(42–51)	(84–108)	
S. bifurcatum	521	22	45	69	114	54	24	4.5	10	40	85	25
	(460–590)	(20–24)	(40–49)	(66–80)	(102–130)	(51–59)	(22–25)	(3.8–5.6)	(9–11)	(33–47)	(77–94)	
S. ceratophorum	706	27	55	92	123	66	26	–	106	45	84	45
	(591–800)	(23–34)	(47–70)	(79–103)	(108–144)	(56–74)	(24–28)		(9–13)	(40–56)	(74–96)	
S. goweni	640	25	51	81	119	67	25	5.4	9	43	77	20
	(531–719)	(21–29)	(32–58)	(69–94)	(109–126)	(59–89)	(22–29)	(4–6)	(6–11)	(27–49)	(48–94)	
S. kandii	707	35	55	86	108	63	21	6.5	11	51	87	20
	(632–833)	(27–48)	(52–60)	(76–100)	(95–127)	(54–74)	(17–24)	(5.5–7)	(9–13.6)	(43–59)	(75–98)	
S. pakistanense	683	27	54	80	113	58	24	6	11	47	91	20
	(649–716)	(24–29)	(49–58)	(76–83)	(108–122)	(53–62)	(21–27)	(5–6)	(10–12)	(42–53)	(87–102)	
S. papillatum	652	24	50	88	110	54	27	5.9	12	46	93	20
	(572–720)	(21–31)	(44–58)	(81–96)	(103–121)	(40–78)	(22–30)	(5–6.4)	(8–15)	(40–52)	(66–121)	
S. riobrave	622	28	56	77	114	54	22	5.4	12	49	105	20
	(361–701)	(27–30)	(51–64)	(74–89)	(109–116)	(46–59)	(20–24)	(4.9–6)	(10–12)	(45–55)	(93–111)	
S. yirgalemense	635	29	51	88	121	62	21	5.2	10	42	83	25
	(548–693)	(24–33)	(45–59)	(82–93)	(115–128)	(57–67)	(20–25)	(4.8–5.9)	(9–11)	(38–48)	(67–98)	

– Data not available.

width of 1.1:1). Calomus distinct, but short. Lamina with two internal ribs, well curved. Velum extending from calomus almost to the end of lamina. Gubernaculum arcuate, *ca* 75% of spicule length, boat-shaped in lateral view, swollen at middle, with prominent narrow neck (Figure 3g). Gubernaculum wings well divided and cuneus pointed (Figure 3g). Tail short and rounded, mucron absent (Figure 3c). Twenty-seven genital papillae comprising 13 pairs and a single midventral papilla located just anterior to cloacal aperatrure. Paired papillae arranged as follows: five pairs subventral precloacal, one pair lateral precloacal, two pairs adcloacal subventral, and five pairs postcloacal (two pair subdorsal and three pairs subventral terminal) (Figures 2g, h).

Second-generation male. General morphology similar to that of first-generation male, but smaller body and tail with a well-developed mucron (Figures 3d and Table 1).

First-generation female. Body usually C-shaped, variable in length and usually coiled on heat relaxation. Head rounded or slightly truncated, bearing six labial and four cephalic papillae, continuous with body contour. Mouth opening circular to slightly triangular. Stoma shallow, subtriangular anteriorly; triradiate internally. Stoma short triangular, *ca* 6–8 μm long and 12–19 μm wide. Excretory pore located anterior to nerve ring at about mid-point of pharynx. Cardia prominent. Gonads amphidelphic, reflexed, always containing many eggs. Vulva opening at mid-body, slightly asymmetrical and in form of a transverse slit, protruding *ca* 20 μm from body contour (Figure 2f), Small epiptygma rarely observed (Figure 3e). Vagina short, leading into paired uteri. Rectum narrow, anal opening distinct. Postanal swelling not observed in most of the mature females (Figure 3h). Lateral field and phasmids not observed. Tail of mature females obese, tail conoid to dome-shaped, bearing two minute projections (Figures 2d and 3h).

Second-generation female. Similar to the first generation in general morphology, but most of the morphometric measurements smaller; for example, body diameter is substantially lower than that of the first-generation females (Table 1). Vulval opening slightly posterior to mid-body (Figure 3f). Tail conical, longer than anal body diameter, with a pointed tip and without mucron. Postanal swelling distinct (Figure 3i).

Taxonomic summary

Type material. Holotype, first-generation male; paratype, infective juveniles, males, and females of first and second generations were mounted on glass slides and deposited at the EPN repository in the

https://doi.org/10.1017/S0022149X23000536 Published online by Cambridge University Press

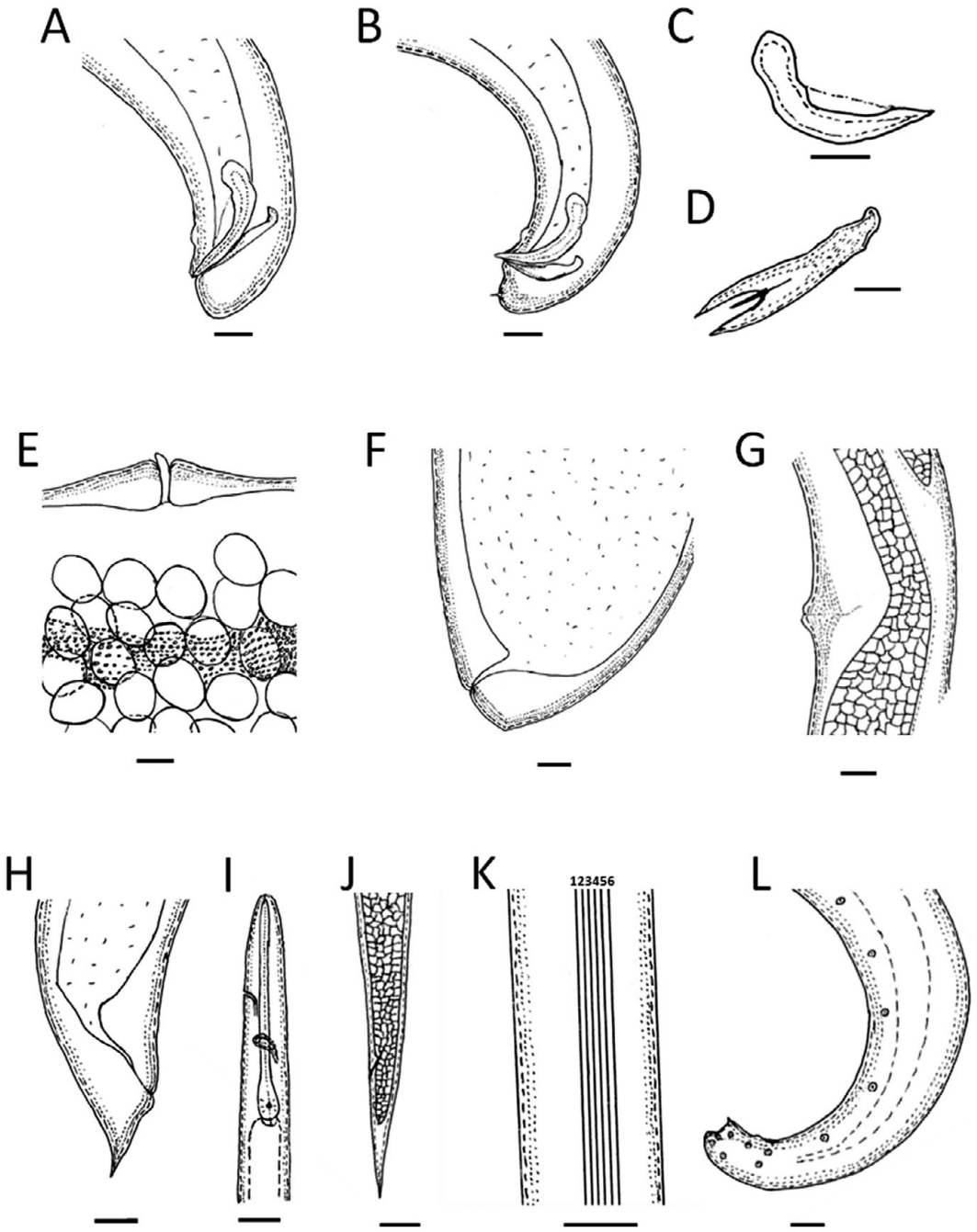

Figure 1. *Steinernema shori* n. sp. line drawings. First-generation male: (a) tail with spicules; Second-generation male: (b) tail with spicules and mucron; (c) spicule; (d) gubernaculum. First-generation female: (e) vulval region; (f) tail. Second-generation female: (g) vulval region; (h) tail. Third-stage infective juvenile: (i) anterior region with excretory pore and nerve ring; (j) tail with anus and hyaline region; (k) lateral field with ridges numbered from 1 to 6. First-generation male: (l) tail with arrangement of genital papillae. Scale bar: (a–c, e–j, l) 20 μm; (d, k) 10 μm.

laboratory of entomopathogenic nematodes, division of germplasm collection and characterization, Indian Council of Agricultural Research (ICAR)-National Bureau Agricultural Insect Resources, Bengaluru, Karnataka, India.

Type host. The natural host is unknown.

Type locality. Steinernema shori n. sp. was recovered by baiting with *G. mellonella* larvae from soil samples collected from the rhizosphere of a Sal (*Shorea robusta*) plantation in Jagdalpur city (19°5′8″N, 81°57′35″E), Bastar District, Chhattisgarh state, India.

Etymology. The specific epithet refers to the *Shorea.*

Diagnosis and relationships

Steinernema shori n. sp. belongs to the "*bicornutum*" group because of the presence of the horn-like structures on the IJ labial region, and the new species is characterized by combination of the morphological and morphometric traits of infective juveniles and adults (Table 1). Infective juvenile is characterised by a small body length of 587 μm (494–671 μm), the position of the excretory pore at 46 μm (43–50 μm), and distance from anterior end to the nerve ring of 72 μm (61–85 μm). Excretory pore located anterior to

https://doi.org/10.1017/S0022149X23000536 Published online by Cambridge University Press

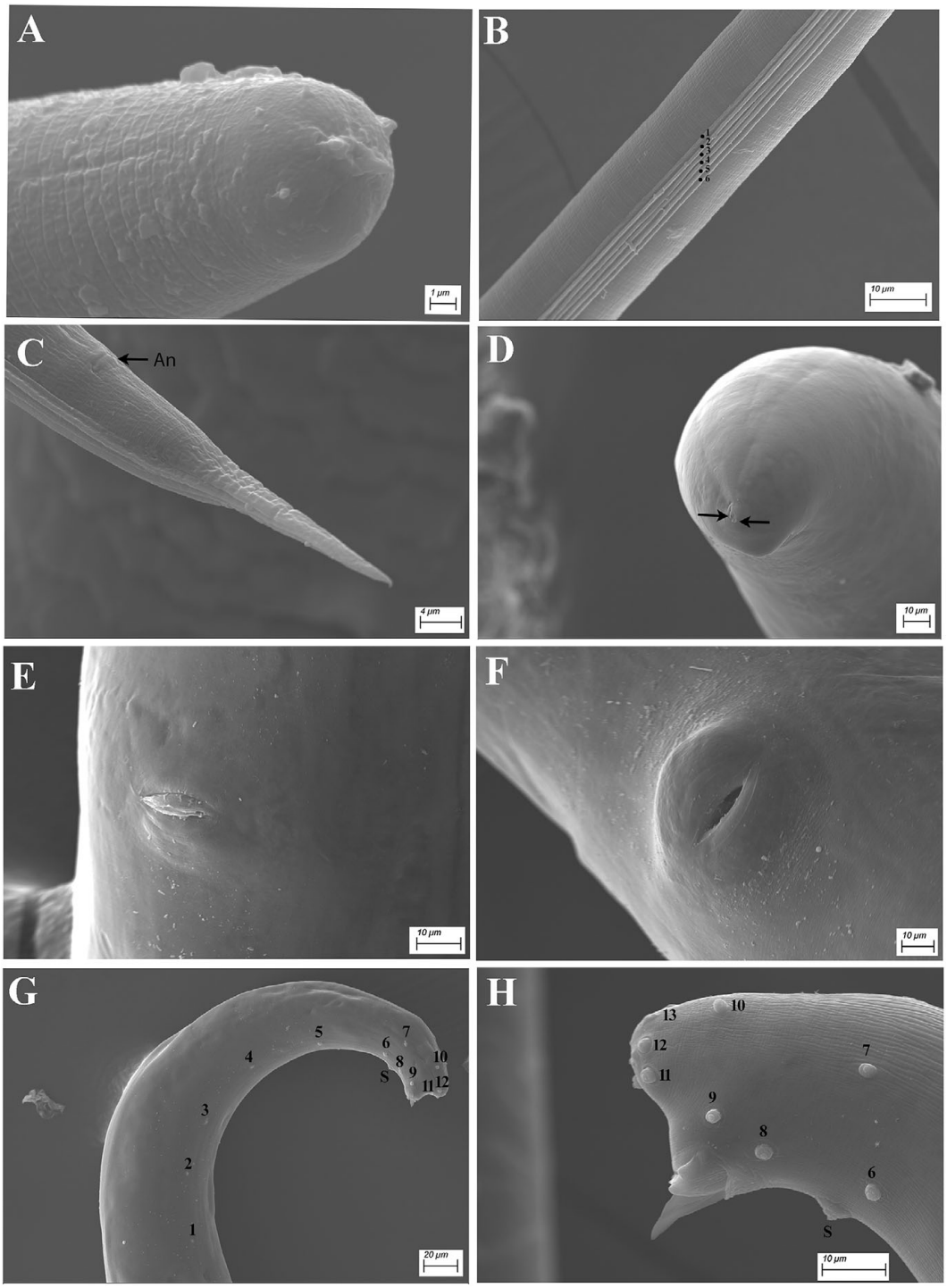

Figure 2. *Steinernema shori* n. sp. SEM photographs. Infective juvenile: (a) head region showing two horn-like structures; (b) lateral field in mid-body (ridges numbered 1–6); (c) tail region with anus (An). First-generation female: (d) tail showing two minute projections (arrows); (e–f) vulval variation. First-generation male: (g) tail with genital papillae (numbered) and a single midventral papilla; (h) tail with part of genital papillae (numbered), spicules.

midpharynx (*D*% = 45) (Table 1). Hyaline layer occupies approximately half of tail length, lateral fields with six ridges in mid-body region forming the formula 2, 6, 2 (Figure 2b). Male spicules moderately curved, with a sharp tip, golden brown in colour, manubrium elongate with a length to width ratio of 1.1:1. First-generation males lacking a mucron on the tail tip while second-generation males bearing a 5 µm (3.1–6.9 µm) mucron on the tail tip. The first-generation males are characterised by very short spicules of 61 µm (53–67 µm) in length (Table 1). Genital papillae with 13 pairs and a single midventral papilla located just anterior to cloacal aperatrure (Figures 2g, h). Both first- and second-generation females possess a moderately protruding vulva but

https://doi.org/10.1017/S0022149X23000536 Published online by Cambridge University Press

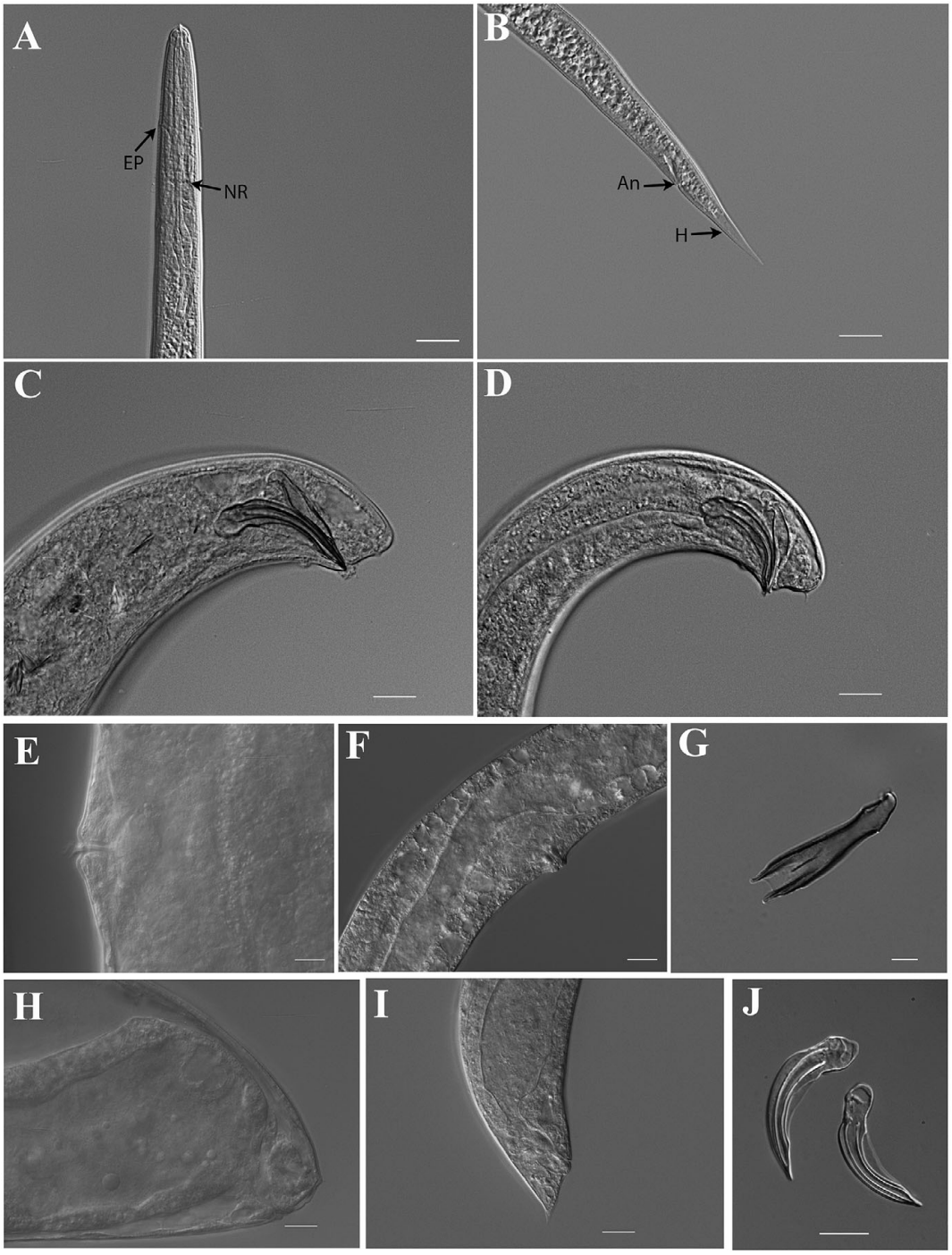

Figure 3. *Steinernema shori* n. sp. LM photographs. Infective juvenile: (a) excretory pore (EP) and nerve ring (NR); (b) tail with anus (AN) and hyaline region (H). First-generation male: (c) tail with spicules and gubernaculum. Second-generation male: (d) tail with spicules, gubernaculum and mucron. First-generation female: (e) vulval region. Second-generation female: (f) vulval region. First-generation male: (g) gubernaculum. First-generation female: (h) tail region. Second-generation female: (h) tail with postanal swelling. First-generation male: (j) spicules. Scale bars: (a–f) 20 μm; (g) 10 μm; (h–j) 20 μm.

postanal swelling observed only in second-generation females (Figure 3i).

Steinernema shori n. sp. can be distinguished from other *Steinernema* species by means of a combination of morphological and morphometric characteristics of males and infective juveniles. Based on these data, *S. shori* n. sp. belongs to the "*bicornutum*" clade within the Steinernematidae family. In the diagnosis, special emphasis will be given to the representatives of "*bicornutum*" clade that are phylogenetically closest relatives of *S. shori* n. sp., namely *S. abbasi* Elawad, Ahmad and Reid; *S. biddulphi* Çimen, Půža, Nermut′, Hatting, Ramakuwela and Hazir; *S. bifurcatum* Fayyaz, Yan, Qui, Han, Gulsher, Khanum and Javed; *S. kandii* Godjo, Afouda, Baimey, Couvreur, Zadji, Houssou, Bert, Willems and Decraemer; *S. pakistanense* Shahina, Anis, Reid, Rowe and Maqbool; and *S. yirgalemense* Nguyen, Tesfamariam, Gozel, Gaugler and Adams.

https://doi.org/10.1017/S0022149X23000536 Published online by Cambridge University Press

Table 3. Comparison of morphometrics of first-generation males of *Steinernema shori* n. sp. with other members of *bicornutum*-group. All the measurements are in μm and in the form: mean (range). Abbreviations as defined in Table 1

Species	SL	GL	ABD	D%	SW%	GS%	n
S. shori n. sp.	61	46	45	51	139	75	20
	(53–67)	(37–54)	(34–52)	(42–63)	(107–190)	(62–90)	
S. abbasi	65	45	43	60	156	70	15
	(57–74)	(35–50)	(37–55)	(51–68)	(107–187)	(58–85)	
S. bicornutum	65	47	109	52	222	72	20
	(53–70)	(38–50)	(80–127)	(50–60)	(218–226)	–	
S. biddulphi	72	44	47	59	153	62	20
	(65–78)	(41–48)	(40–59)	(52–69)	(126–192)	(54–70)	
S. bifurcatum	69	39	48	48	1.4	0.59	25
	(60–85)	(30–49)	(45–56)	(42–58)	(1.2–1.7)	(0.51–0.74)	
S. ceratophorum	71	40	52	51	140	60	35
	(54–90)	(25–45)	(45–70)	(33–69)	(100–200)	(40–80)	
S. goweni	55	35	40	42	146	64	20
	(50–57)	(30–40)	(31–48)	(28–59)	(105–208)	(49–79)	
S. kandii	67	36	53	63	129	55	20
	(57–75)	(26–46)	(36–66)	(38–77)	(96–175)	(41–65)	
S. pakistanense	68	41	36	60	189	60	20
	(62–73)	(36–48)	(32–40)	(50–60)	(100–220)	(50–60)	
S. papillatum	58	31	34	54	156	59	20
	(47–66)	(23–36)	(26–44)	(43–65)	(125–194)	(48–70)	
S. riobrave	67	51	59	71	114	76	10
	(63–75)	(48–56)	(50–64)	(60–80)	–	–	
S. yirgalemense	64	48	38	58	171	74	20
	(51–77)	(42–54)	(32–45)	(50–66)	(121–213)	(65–85)	

– Data not available.

Table 4. Number of base differences (below diagonal) and pairwise nucleotide similarities (above diagonal) of the ITS and D2–D3 segments of the rDNA among species of the "*bicornutum*" group. Data for *Steinernema shori* n. sp. in bold

	ITS	1	2	3	4	5	6	7	8	9	10	11	12	13
1	***S. shori* n. sp. OR194554**		**78.6**	**76.1**	**82.2**	**79.7**	**74.8**	**77.3**	**78.5**	**78.3**	**77.3**	**76**	**78.8**	**72.8**
2	*S. abbasi* EF469773	**176**		97.2	81.6	79.2	73	74.7	76.4	74.3	77	75.1	78.4	71.9
3	*S. kandii* KY228996	**178**	21		78.9	77.3	73.2	73.2	73.8	71.9	75.1	75.1	76.3	71.9
4	*S. yirgalemense* AY748450	**169**	148	154		78	72.2	76.1	77.6	76.9	76.6	75.2	78.2	70
5	*S. biddulphi* KT373857	**190**	168	166	202		87.9	89.1	76.2	77.3	76.1	75.1	78	71.8
6	*S. bifurcatum* JX989267	**200**	199	199	216	96		98.9	71.5	72.2	70.4	72.4	70.8	66.5
7	*S. pakistanense* AY748449	**220**	207	199	227	103	9		73.9	75.4	72.5	72.4	74.4	66.1
8	*S. goweni* KR781038	**194**	193	194	198	210	224	238		81.5	83.1	84.8	80.9	74.2
9	*S. riobrave* DQ835613	**206**	208	206	215	207	216	234	173		85.3	87	79.7	73.9
10	*S. papillatum* KJ913707	**190**	187	177	192	197	219	232	147	127		91.2	79.8	74.7
11	*S. ralatorei* KP036472	**183**	180	185	185	186	211	211	121	103	68		79.3	75.9
12	*S. ceratophorum* AY230165	**202**	174	173	200	199	222	239	174	192	168	158		85.6
13	*S. bicornutum* AY171279	**195**	200	197	211	200	241	244	193	191	186	176	109	

(*Continued*)

https://doi.org/10.1017/S0022149X23000536 Published online by Cambridge University Press

Table 4. (*Continued*)

	ITS	1	2	3	4	5	6	7	8	9	10	11	12	13
	D2D3	**1**	**2**	**3**	**4**	**5**	**6**	**7**	**8**	**9**	**10**	**11**	**12**	**13**
1	***S. shori* n. sp. OR194555**		**90.3**	**90.7**	**91.2**	**90.4**	**87.5**	**87.5**	**88.8**	**87.8**	**88.2**	**89.5**	**90.4**	**91.6**
2	*S. abbasi* AF331890	**83**		98.3	94.6	89.1	95.1	86.4	88.8	87.0	89.7	88.7	89.2	89.9
3	*S. kandii* MG495398	**55**	10		93.2	90.9	98.3	88.3	89.8	88.1	88.5	89.8	89.5	90.8
4	*S. yirgalemense* AY748451	**52**	32	39		90.9	94.6	89.6	91.2	90.5	89.8	91.5	90.7	91.6
5	*S. biddulphi* KT580950	**81**	90	54	54		87.6	94.3	88.5	86.9	89.0	89.2	88.8	89.4
6	*S. bifurcatum* JQ838179	**109**	42	10	32	104		83.0	87.9	84.2	89.8	85.4	85.5	86.1
7	*S. pakistanense* MF289982	**105**	115	66	60	46	143		86.0	85.4	86.9	86.8	86.1	87.9
8	*S. goweni* KR781039	**93**	91	60	52	96	101	112		93.5	94.3	95.3	91.4	91.8
9	*S. riobrave* GU177834	**106**	111	70	56	110	138	123	54		95.4	95.9	88.9	89.4
10	*S. papillatum* KM229421	**72**	62	67	60	67	62	77	35	28		97.5	89.7	90.7
11	*S. ralatorei* KP036475	**91**	98	60	50	90	128	111	39	36	15		90.2	90.6
12	*S. ceratophorum* MW029452	**84**	93	62	55	94	128	118	72	97	63	86		95.6
13	*S. bicornutum* AF331904	**72**	88	53	50	87	120	102	67	91	56	82	38	

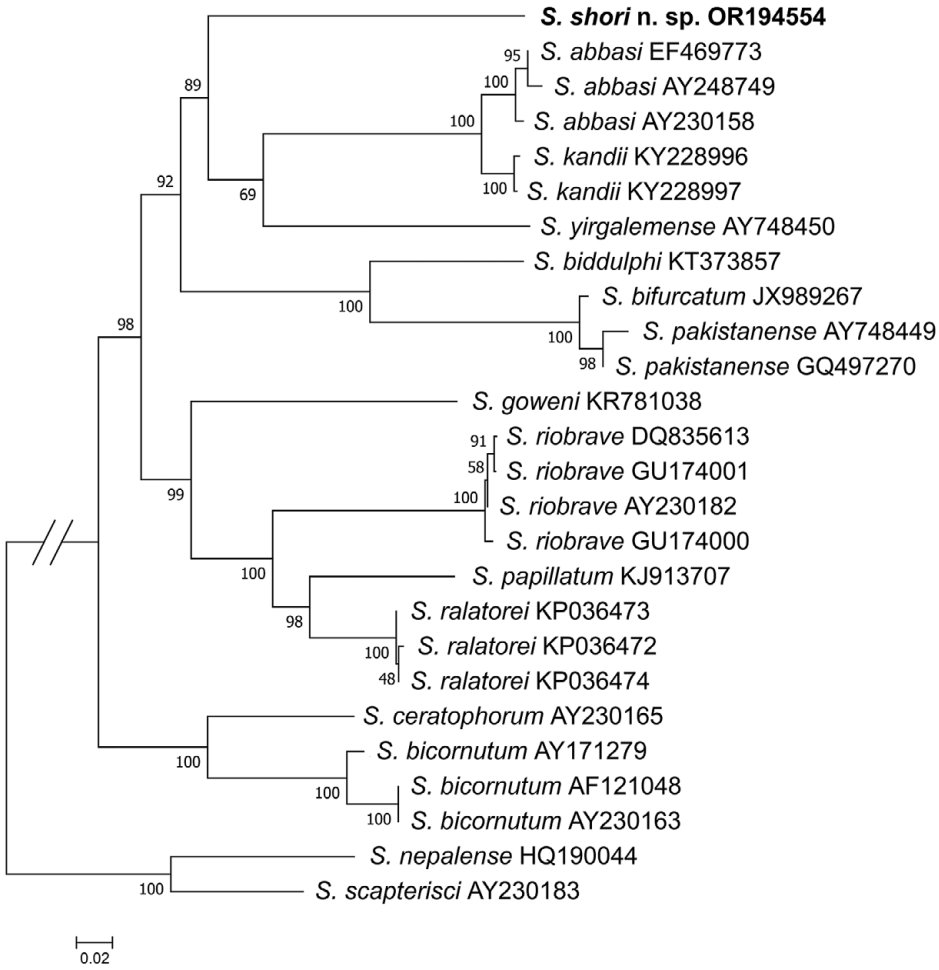

Figure 4. Phylogenetic relationships of *Steinernema shori* n. sp. and other members of the *bicornutum*-group of *Steinernema* based on analysis of ITS rDNA regions. *Steinernema nepalense* and *S. scapterisci* were used as outgroup taxa. The percentages of replicate trees in which the associated taxa clustered together in the bootstrap test (10 000 replicates) are shown next to the branches. Branch lengths indicate evolutionary distances and are expressed in the units of number of base differences per site.

https://doi.org/10.1017/S0022149X23000536 Published online by Cambridge University Press

The first-generation males of *S. shori* n. sp. can be distinguished from all species from the "*bicornutum*" group by the presence of a total of 27 genital papillae in all individuals. Other species have a total of 23 or 25 papillae, with the exception of *S. abbasi* and *S. goweni*, where both males with 25 and 27 papillae are present. The first-generation males of *S. shori* n. sp. can be further distinguished from other species based on *D*% = 51 µm (42–63 µm), which is higher in comparison to *S. bifurcatum* 48 µm (42–58 µm), but lower in comparison with *S. abbasi* 60 µm (51–68 µm), *S. biddulphi* 59 µm (52–69 µm), *S. kandii* 63 µm (38–77 µm), *S. pakistanense* 60 µm (50–60 µm), and *S. yirgalemense* 58 µm (50–66 µm). The *SW*% ratio of *S. shori* n. sp. of 139 µm (107–190 µm) is higher in comparison to *S. kandii* 129 µm (96–175 µm) and lower than that of *S. abbasi* 156 µm (107–187 µm) and S. *yirgalemense* 171 µm (121–213 µm). The *GS*% ratio of *S. shori* n. sp. of 75 µm (62–90 µm) is higher in comparison to *S. abbasi* 70 µm (58–85 µm), S. *biddulphi* 62 µm (54–70 µm), *S. kandii* 55 µm (41–65 µm), S. *pakistanense* 60 µm (50–60 µm), and S. *yirgalemense* 74 µm (65–85 µm). Furthermore, first generation-males of *S. shori* n. sp. differ from those of *S. abbasi, S. biddulphi, S. bifurcatum, S. kandii, S. pakistanense,* and *S. yirgalemense* in possessing shorter spicules length of 61 µm (53–67 µm) (Table 3).

Infective juveniles (IJ) of *S. shori* n. sp. with a body length of 587 µm (494–671 µm), are longer those of *S. abbasi* and *S. bifurcatum* with lengths of 541 µm (510–620 µm) and 521 µm (460–590 µm), respectively, and smaller than those of *S. kandii* with length of 707 µm (632–833 µm), *S. pakistanense* (683 µm (649–716 µm)), and *S. yirgalemense* (635 µm (548–693 µm)). The IJs of *S. shori* n. sp. differ from those of *S. abbasi, S. biddulphi, S. kandii, S. pakistanense,* and *S. yirgalemense* in possessing shorter distance from anterior end to excretory pore at 46 µm (43–50 µm). The b ratio of *S. shori* n. sp. of 5.8 µm (5.1–6.7 µm) is greater in comparison to *S. yirgalemense* 5.2 µm (4.8–5.9 µm) and c ratio 11 µm (10–12 µm), which is also greater in comparison to *S. yirgalemense* 10 µm (9–11 µm). The IJs of *S. shori* n. sp. can also be distinguished from other closely related species of "*bicornutum*" group based on the *D*% of IJs of *S. shori* n. sp., which is also higher than in *S. bifurcatum* and *S. yirgalemense* (45 µm (43–50 µm) vs 40 µm (33–47 µm) and 42 µm (38–48 µm), respectively. The IJs of *S. shori* n. sp. can be distinguished from *S. biddulphi, S. kandii,* and *S. yirgalemense* by the distance from anterior end to nerve ring of 72 µm (61–85 µm) vs 92 µm (84–103 µm), 86 µm (76–100 µm), and 88 µm (82–93 µm), respectively. The esophagus of *S. shori* n. sp. IJs of 102 µm (93–116 µm) is longer than that of *S. abbasi* 89 µm (85–92 µm) yet shorter than in *S. biddulphi* and *S. yirgalemense,* with

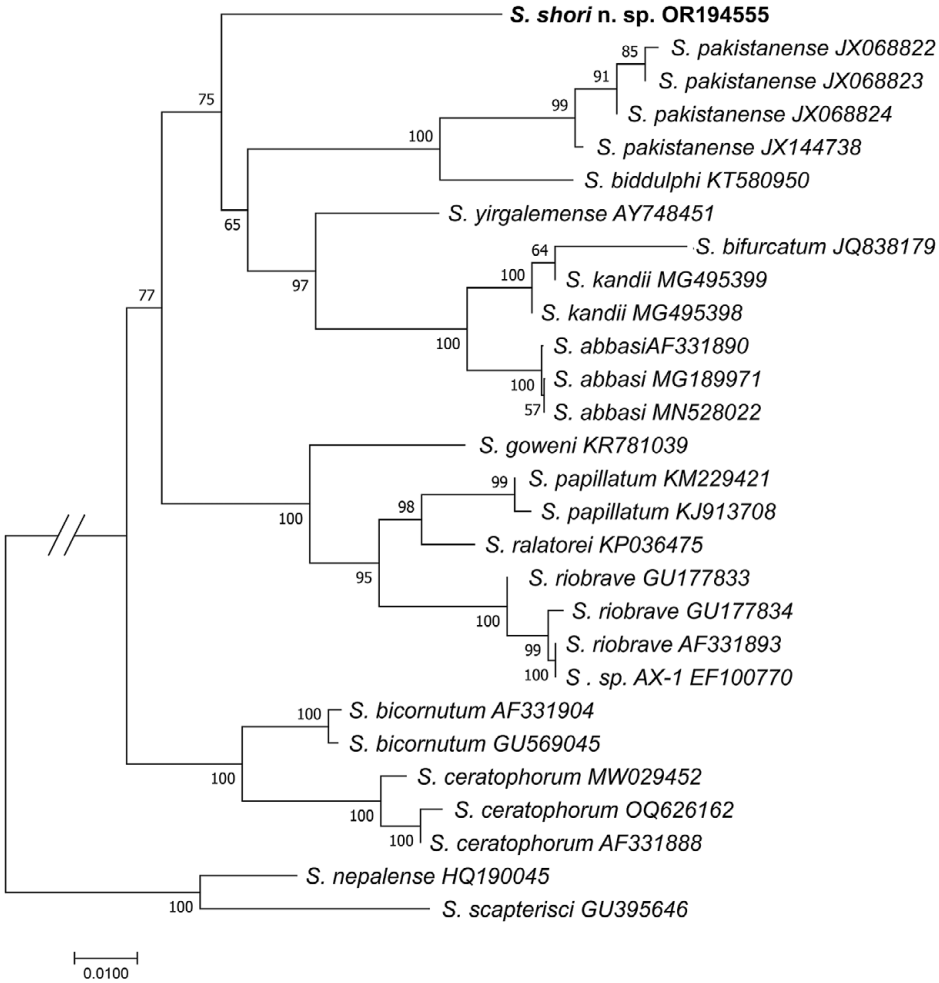

Figure 5. Phylogenetic relationships of *Steinernema shori* n. sp. and other members of the *bicornutum*-group of *Steinernema* based on analysis of D2–D3 expansion segments of the 28S rDNA. *Steinernema nepalense* and *S. scapterisci* were used as outgroup taxa. The percentages of replicate trees in which the associated taxa clustered together in the bootstrap test (10 000 replicates) are shown next to the branches. Branch lengths indicate evolutionary distances and are expressed in the units of number of base differences per site.

https://doi.org/10.1017/S0022149X23000536 Published online by Cambridge University Press

esophagus lengths of 118 µm (111–126 µm) and 121 µm (115–128 µm), respectively (Table 2).

Molecular characterization and phylogenetic analysis

Steinernema shori n. sp. is characterized by the sequences of the ITS and D2–D3 regions of the rDNA (Table 4) and mitochondrial COI gene. The sequences of *S. shori* n. sp. differ substantially from all other species of the "*bicornutum*" group. The sequences of ITS and D2–D3 regions of *S. shori* n. sp. are most similar to those of *S. yirgalemense* with similarities of 82.2% and 91.2%, respectively. Phylogenetic analyses based on the ITS and D2–D3 regions clearly confirm *S. shori* n. sp. as a member of "*bicornutum*" group. The ITS tree shows *S. shori* n. sp. as a sister taxon to the group formed by a pair of *S. abbasi* and *S. kandii* and *S. yirgalemense* with a high bootstrap support (Figure 4). The analysis based on the D2–D3 region of the rDNA places *S. shori* n. sp. as a sister taxon of the group formed by *S. abbasi, S. kandii, S. yirgalemense, S. pakistanense, S. bifurcatum* and *S. biddulphi* (Figure 5). Unfortunately, there are not enough COI sequences of "*bicornutum*" group members available in the NCBI Genbank database, with the mitochondrion sequence attributed to *S. abbasi* (NC_039926.1) obviously belonging to *S. carpocapsae.* Nevertheless, the BLAST search shows that the COI sequence of *S. shori* n. sp. most resembles to that of *S. borjomiense* (LT963444) with similarity of 90.88%.

Bacterial symbiont

The sequence analysis of the 16S rDNA, *recA*, and *gyrB* genes show that the bacterial symbiont of *S. shori* n. sp. differs substantially from other *Xenorhabdus* species (Table 5 and Figure 6) and likely belongs to a new, as yet undescribed *Xenorhabdus* species. According to the BLAST search, the 16S sequence of *Xenorhabdus* sp. NBAIRS80 is closest to *Xenorhabdus thuongxuanensis*, *Xenorhabdus budapestensis*, and *Xenorhabdus indica* with similarities of

Table 5: Number of base differences (below diagonal) and pairwise nucleotide similarities (above diagonal) of the *recA* and *gyrB* genes of *Xenorhabdus* sp. NBAIRS80 and related *Xenorhabdus* species

RecA		1	2	3	4	5	6	7
1	*Xenorhabdus* sp. *recA* OR232178		96.6	96.0	95.7	88.5	88.5	86.1
2	*X. indica* FJ823421	22		97.2	96.3	89.5	89.8	86.7
3	*X. budapestensis* FJ823418	26	18		97.4	89.9	90.4	86.5
4	*X. cabanillasii* FJ823422	28	24	17		89.9	90.1	87.2
5	*X. stockiae* FJ823425	74	68	65	65		92.4	88.4
6	*X. innexi* FJ823423	74	66	62	64	49		86.1
7	*X. bovienii* FJ823426	90	86	87	83	75	90	
GyrB		**1**	**2**	**3**	**4**	**5**	**6**	**7**
1	*Xenorhabdus* sp. *gyrB* OR232179		96.5	97.0	96.9	87.5	88.0	86.5
2	*X. indica* EU934538	30		97.2	97.3	88.1	88.2	86.1
3	*X. budapestensis* EU934535	26	24		98.3	88.7	89.1	87.3
4	*X. cabanillasii* EU934537	27	23	15		88.8	89.0	87.0
5	*X. innexi* EU934540	108	103	98	97		93.1	87.0
6	*X. stockiae* EU934542	104	102	94	95	60		87.0
7	*X. bovienii* EU934530	117	120	110	112	112	112	

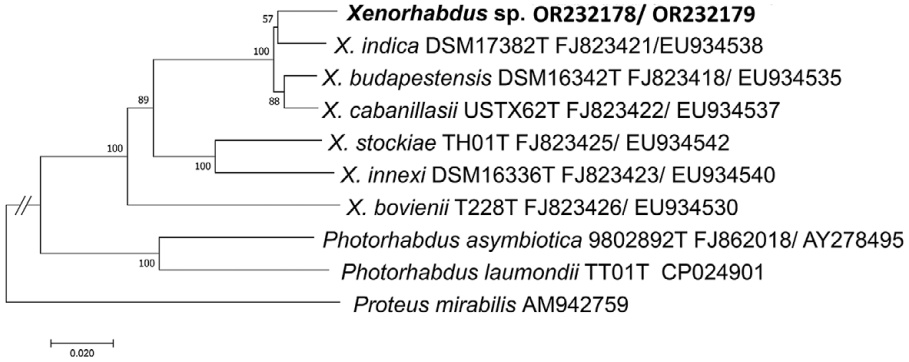

Figure 6. Phylogenetic relationships of *Xenorhabdus* sp. strain NBAIRS80 isolated from *Steinernema shori* n. sp. and other closely related species of *Xenorhabdus*, based on the analysis of concatenated *rec*A and *gyr*B gene sequences. The percentages of replicate trees in which the associated taxa clustered together in the bootstrap test (1000 replicates) are given at each node. Branch lengths indicate evolutionary distances and are expressed in units of number of base differences per site.

https://doi.org/10.1017/S0022149X23000536 Published online by Cambridge University Press

ca 97.5–97.7%. Pairwise distance analysis of the *recA* and *gyrB* gene sequences demonstrated that the sequences of bacterial symbiont of *S. shori* n. sp. are most similar to those of *X. indica* and *X. cabanillasii* with similarities of *ca* 96–97% (Table 5). The phylogenetic tree based on concatenated sequences of the *recA* and *gyrB* genes demonstrate that *Xenorhabdus* sp. from *S. shori* n. sp. is closely related to *X. indica*, *X. budapestensis*, and *X. cabanillasii.*

Supplementary material. The supplementary material for this article can be found at http://doi.org/10.1017/S0022149X23000536.

Acknowledgements. The authors thank the Director, National Bureau of Agricultural Insect Resources, Bengaluru, for providing the research facilities and the Central Instrumentation Facility (CIF), University of Agricultural Sciences, Bangalore (UASB), GKVK, Bengaluru. We thank the National Higher Education Project (NAHEP) of the Indian Council of Agricultural Research, New Delhi, for supporting the CIF facility and Dr Nataraja Karaba N, Head of the Central Instrumentation Facility, for expert assistance with the analysis.

Financial support. This work was supported by the Indian Council of Agricultural Research (ICAR), New Delhi, ICAR-National Bureau of Agricultural Insect Resources, Bengaluru, Karnataka, and Indira Gandhi Krishi Vishwavidyalaya, Raipur, Chhattisgarh.

Competing interest. None.

Ethical standard. The authors assert that all procedures contributing to this work comply with the ethical standards of the relevant national and institutional guides on the care and use of laboratory animals.

References

Akhurst RJ (1980). Morphological and functional dimorphism in *Xenorhabdus* spp. bacteria symbiotically associated with the insect pathogenic nematodes *Neoaplectana* and *Heterorhabditis*. *Journal of General Microbiology* **121**, **2**, 303–309. https://doi.org/10.1099/00221287-121-2-303

Altschul SF, **Madden TL**, **Schäffer AA**, **Zhang J**, **Miller W**, **Lipman DJ** (1997). Gapped BLAST and PSI-BLAST: a new generation of protein database search programs. *Nucleic Acids Research* **25**, **17**, 3389–3402. https://doi.org/10.1093/nar/25.17.3389

Bedding RA, **Akhurst RJ** (1975). A simple technique for the detection of insect parasitic rhabditid nematodes in soil. *Nematologica* **21**, **1**, 109–110. https://doi.org/10.1163/187529275X00419

Bhat AH, **Machado AR**, **Abolafia J**, **Askary TH**, **Půža V**, **Ruiz-Cuenca AN**, **Ameen F**, **Rana A**, **Sayed S**, **Al-Shuraym LA** (2023). Multigene sequence-based and phenotypic characterization reveals the occurrence of a novel entomopathogenic nematode species, Steinernema anantnagense *n. sp.* Journal of Nematology, **55**, **1**, 20230029. https://doi.org/10.2478/jofnem-2023-0029

Cabanillas HE, **Poinar Jr GO**, **Raulston JR** (1994). *Steinernema riobravis* n. sp. (Rhabditida: Steinernematidae) from Texas. *Fundamental and Applied Nematology* **17**, 123–131.

Cimen H, **Půža V**, **Nermut' J**, **Hatting J**, **Ramakuwela T**, **Hazir S** (2016). *Steinernema biddulphi* n. sp., a new entomopathogenic nematode (Nematoda: Steinernematidae) from South Africa. *Journal of Nematology* **48**, **3**, 148–158. https://doi.org/10.21307/jofnem-2017-022

De Maeseneer J, **D' Herde J** (1963). Méthodes utilisées pour l'étude des anguillules libres du sol. *Revue de l' Agriculture Bruxelles* **16**, 441–447.

Elawad S, **Ahmed W**, **Reid AP** (1997). *Steinernema abbasi* sp. n. (Nematoda: Steinernematidae) from the Sultanate of Oman. *Fundamental and Applied Nematology* **20**, **5**, 435–442.

Fayyaz S, **Yan X**, **Qiu L**, **Han R**, **Gulsher M**, **Khanum TA**, **Javed S** (2014). A new entomopathogenic nematode, *Steinernema bifurcatum* n. sp. (Rhabditida: Steinernemati- dae) from Punjab, Pakistan. *Nematology* **16**, **7**, 821–836. https://doi.org/10.1163/15685411-00002811

Godjo A, **Afouda L**, **Baimey H**, **Couvreur M**, **Zadji L**, **Houssou G**, **Wimbert, Willems A**, **Decraemer W** (2019). *Steinernema kandii* n. sp. (Rhabditida: Steinernematidae), a new entomopathogenic nematode from northern Benin. *Nematology* **21**, **2**, 107–128. https://doi.org/10.1163/15685411-00003201

Grifaldo-Alcantara PF, **Alatorre-Rosas R**, **Segura-León O**, **Hernandez-Rosas F** (2017). *Steinernema ralatorei* n. sp. isolated from sugarcane areas at Veracruz, Mexico. *Southwestern Entomologist* **42**, **1**, 171–190. https://doi.org/10.3958/059.042.0117

Hall TA (1999). BioEdit: a user-friendly biological sequence alignment editor and analysis program for Windows 95/98/NT. *Nucleic Acids Symposium Series* **41**, 95–98.

Hominick WM (2002). Biogeography. In Gaugler R (ed), *Entomopathogenic Nematology*. Wallingford, UK: CABI Publishing, 115–143.

Hooper DJ (1970). Handling, fixing, staining, and mounting nematodes. In Southey JF (ed) *Laboratory Methods for Work with Plant and Soil Nematodes*, 5th edition. London: Her Majesty's Stationery Office, 39–54.

Jian H, **Reid AP**, **Hunt DJ** (1997). *Steinernema ceratophorum* n. sp. (Nematoda: Steinernematidae), a new entomopathogenic nematode from north-east China. *Systematic Parasitology* **37**, 115–125. https://doi.org/10.1023/A:1005798031746

Kanzaki N, **Futai K** (2002). A PCR primer set for determination of phylogenetic relationships of *Bursaphelenchus* species within the *xylophilus* group. *Nematology* **4**, **1**, 35–41. https://doi.org/10.1163/156854102760082186

Kaya HK, **Stock SP** (1997). Techniques in insect nematology. In Lacey I (ed), *Manual of Techniques in Insect Pathology*. San Diego: Academic Press, 313–314.

Khatri-Chhetri HB, **Waeyenberge I**, **Spiridonov SE**, **Manadhar HM**, **Moens M** (2011). Two new species of *Steinernema* Travassos, 1927 with short IJ from Nepal. *Russian Journal of Nematology* **19**, **1**, 53–74.

Kumar S, **Stecher G**, **Tamura K** (2016). MEGA7: molecular evolutionary genetics analysis version 7.0 for bigger datasets. *Molecular Biology and Evolution* **33**, **7**, 1870–1874. https://doi.org/10.1093/molbev/msw054

Nei M, **Kumar S** (2000). *Molecular Evolution and Phylogenetics*. New York: Oxford University.

Nguyen KB (2007). Methodology, morphology and identification. In Nguyen KB, Hunt DJ (eds.) *Entomopathogenic Nematodes: Systematics, Phylogeny and Bacterial Simbionts. Nematology Monographs & Perspectives* **5**. Leiden: Brill, 59–119.

Nguyen KB, **Smart Jr GC** (1990). *Steinernema scapterisci* n. sp. (Rhabditida: Steinernematidae). *Journal of Nematology* **22**, **2**, 187–199.

Nguyen KB, **Smart Jr GC** (1995). Scanning electron microscope studies of *Steinernema glaseri* (Nematoda: Steinernematidae). *Nematologica* **41**, 183–190.

Nguyen KB, **Smart Jr GC** (1997). Scanning electron microscope studies of spicules and gubernacula of *Steinernema* spp. (Nemata: Steinernematidae). *Nematologica* **43**, 465–480.

Nguyen KB, **Tesfamariam M**, **Gozel U**, **Gaugler R**, **Adams BJ** (2004). *Steinernema yirgalemense* n. sp. (Rhabditida: Steinernematidae) from Ethiopia. *Nematology* **6**, 839–856. https://doi.org/10.1163/1568541044038605

Patil J, **Linga V**, **Mhatre PH**, **Gowda MT**, **Rangasamy V**, **Půža V** (2023). *Steinernema indicum* n. sp., a new entomopathogenic nematode (Nematoda: Steinernematidae) from India. *Nematology* **25**, **7**, 815–833. doi: https://doi.org/10.1163/15685411-bja10258

Půža V (2015). Control of insect pests by entomopathogenic nematodes. In Lugtenberg B (ed), *Principles of Plant-Microbe Interaction, Microbes for Sustainable Agriculture*. Springer Cham Heidelberg: New York Dordrecht London., 175–183.

Rzhetsky A, **Nei M** (1992). A simple method for estimating and testing minimum evolution trees. *Molecular Biology and Evolution* **9**, **5**, 945–967. https://doi.org/10.1093/oxfordjournals.molbev.a040771

Saitou N, **Nei M** (1987). The neighbor-joining method: a new method for reconstructing phylogenetic trees. *Molecular Biology and Evolution* **4**, **4**, 406–425. https://doi.org/10.1093/oxfordjournals.molbev.a040454

San-Blas E, **Morales-Montero P**, **Portillo E**, **Nermut' J**, **Půža V** (2016). *Steinernema goweni* n. sp. (Rhabditida: Steinernematidae), a new entomopathogenic nematode from Zulia State, Venezuela. *Zootaxa* **4067**, 200–214.

San-Blas E, **Portillo E**, **Nermut' J**, **Půža V**, **Morales-Montero P** (2015). *Steinernema papillatum* n. sp. (Rhabditida: Steinernematidae), a new

entomopathogenic nematode from Venezuela. *Nematology* **17**, **9**, 1081–1097. https://doi.org/10.1163/15685411-00002925

Seinhorst JW (1959). A rapid method for the transfer of nematodes from fixative to anhydrous glycerin. *Nematologica* **4**, **1**, 67–69. https://doi.org/10.1163/187529259X00381

Shahina F, **Anis M**, **Reid AP**, **Rowe J**, **Maqbool M** (2001). *Steinernema pakistanense* sp. n. (Rhabditida: Steinernematidae) from Pakistan. *International Journal of Nematology* **11**, **1**, 124–133.

Tailliez P, **Laroui C**, **Ginibre N**, **Paule A**, **Pagès S**, **Boemare N** (2010). Phylogeny of *Photorhabdus* and *Xenorhabdus* based on universally conserved protein-coding sequences and implications for the taxonomy of these two genera. Proposal of new taxa: *X. vietnamensis* sp. nov., *P. luminescens* subsp. *caribbeanensis* subsp. nov., *P. luminescens* subsp. *hainanensis* subsp. nov., *P. temperata* subsp. *khanii* subsp. nov., *P. temperata* subsp. *tasmaniensis* subsp. nov., and the reclassification of *P. luminescens* subsp. *thracensis* as *P. temperata* subsp. *thracensis* comb. nov. *International Journal of Systematic and Evolutionary Microbiology* **60**, Pt. **8**, 1921–1937. https://doi.org/10.1099/ijs.0.014308-0

Tallósi B, **Peters A**, **Ehlers R-U** (1995). *Steinernema bicornutum* sp. n. (Rhabditida: Steinernematidae) from Vojvodina, Yugoslavia. *Russian Journal of Nematology* **3**, **2**, 71–80.

Vrain TC, **Wakarchuk DA**, **Levesque AC**, **Hamilton RI** (1992). Intraspecific rDNA restriction fragment length polymorphism in the *Xiphinema americanum* group. *Fundamental and Applied Nematology* **15**, **6**, 563–573.

Weisburg WG, **Barns SM**, **Pelletier DA**, **Lane DJ** (1991). 16S ribosomal DNA amplification for phylogenetic study. *Journal of Bacteriology* **173**, **2**, 697–703. https://doi.org/10.1128/jb.173.2.697-703.1991

White GF (1927). A method for obtaining infective juvenile nematode larvae from cultures. *Science* **66**, **1709**, 302–303. https://doi.org/10.1126/science.66.1709.302-a

https://doi.org/10.1017/S0022149X23000536 Published online by Cambridge University Press